Chalcogenide Letters Vol. 16, No. 7, July 2019, p. 343 - 349

INCREASING THE POWER FACTOR BY Sb DOPED $Tl_{10-x}Sb_xTe_6$ IN CHALCOGENIDE SYSTEM

W. M. KHAN[a*], W. H. SHAH[a], S. SHAH[a], S. KHAN[a], W. A. SYED[a],
N. AHMAD[a], A. SAFEEN[b], K. SAFEEN[b]
[a]*Department of Physics, Faculty of Basic and Applied Sciences, International Islamic University, Islamabad, Pakistan*
[b]*Department of Physics, Abdul Wali Khan University, Mardan, Pakistan*

The nano-particles system which is Thallium antimony telluride $Tl_{10-x}Sb_xTe_6$ with different doping with concentration of Sb (x = 1.00, 1.250, 1.500, 1.750, 2.00) were synthesized by solid state reaction method and then the nano-particles from the ingot by ball milling techniques. X-rays diffraction analysis has defined the phase purity of the system, as there is no extra peaks were observed. EDX spectroscopy result confirmed the elemental composition of $Tl_{10-x}Sb_xTe_6$. It is increasing thermal properties as the Sb is doping in the nano-system. While the electrical conductivity (σ) decreased in nano system otherwise the Seebeck coefficient (S) is increased. The different behavior of See-beck co-efficient and electrical conductivity which cause to increase the power factor. Our present study to show that the use of $Tl_{10-x}Sb_xTe_6$ is best nano-particles for thermos-electric generator.

(Received March 21, 2019; Accepted July 16, 2019)

Keywords: Tellurium Telluride Nano-Particles, Sb doping, See-beck co-efficient, Electrical conductivity, Power factor

1. Introduction

It is statistical results show that up to 60% of energy is losing in vain worldwide, most in the form of waste heat. High value of performance which is thermoelectric (TE) materials that is directly and inversely change heat energy to electrical energy have thus draw growing attentions of governments and research institutes [1]. Thermoelectric system is an environment-friendly energy conversion technology with the advantages of small size, high reliability, no pollutants and feasibility in a wide temperature range. However, the efficiency of thermoelectric devices is not high enough to rival the Carnot efficiency [2, 3].

Many new thermoelectric materials or new material with which have high performance have been found such as skutterudites with high scattering rates of phonons [4,5], silicon nanowires [6,7], TE thin films [8], and nanostructured bismuth antimony telluride bulk alloys [9]. It was thinking that high barriers and extremely degenerately doped superl-attices must achieve significant increases in thermos-electric power factor over bulk materials [10]. It was revised that electron transport which are perpendicular to the barrier and investigated that large number of degenerate doped semiconductor or metal super-lattices could achieve which shows the power factors higher than the bulk and determined that non-maintenance of transverse momentum can have a large effect (especially in the case of metal super-lattices) by increasing the number of electrons contributing to conduction by thermionic emission [11].

The See-beck co-efficient for different metals and largely doped semiconductors is determined. The equation is related by the power factor, which is directly proportional to the See-beck coefficient squared, we determined that increasing the See-beck coefficient by having their high effective mass and low carrier concentration, which is in the semiconducting region, is need in a thermoelectric material. Ionic compounds will give us high effective mass with low mobility, while semiconductors with small electro-negativity differences have high mobility and low

---

[*] Corresponding author: waqaskhanrwp@yahoo.com

effective mass. The ideal situation is having high effective mass and high mobility, but this is extremely difficult to tune in a material. One has to compromise one for the other, and there are reports of compounds showing promising thermoelectric material at both ends of the spectrum. Chalcogenides (group 16 10 elements) and silicon-germanium show good TE properties, with the former exploiting high effective mass to achieve a high power factor and the high carrier mobility [12].

2. Experimental section

$Tl_{10-x}Sb_xTe_6$ compound (where x=1.00, 1.250, 1.50, 1.750, 2.0) has been prepared by solid state reaction method from the Sb doped element with different concentration of respective elements (Tl granules, 99.4%; Sb powder, 99.5% and Te broken ingots, >99.99%), with different masses of samples were measured between 60 mg and 120 mg. $Tl_{10-x}Sb_xTe_6$ system was prepared by heating different elements of Tl, Sb and Te in their stoichiometric molar ration and put in a silica tube (approx.10^{-3}mbar) stored in an argon-filled glove box to prevent it from the reaction of other environmental elements. The silica tubes were coated under H_2/O_2 flame. All samples were gradually heated in a furnace with appropriate temperature the profile for these compound is (12 h-650 K- 24 h-650 K 60 h- 650 K and cooled down to 550 K within 100 h). When the reaction mixture was inhomogeneous after heating, then again placed in a silica tube in the argon filled glove box and put in heat furnace for one week. Keeping the process continues until desired homogeneous compound were obtained. The prepared ingot was then put in the Ball milling machine to produce nanoparticles of different sizes as mentioned below. It is a process where a powder mixture placed in the ball mill is subjected to high-energy collision from the balls to fabricate nano-particles.

3. Result and discussion

Fig. 1 shows the powder XRD spectrum of the $Tl_{10-x}Sb_xTe_6$ with different doping concentration (x = 1.0, 1.250, 1.50, 1.750, 2.0). In the XRD patterns, the strongest intensity of the (213) diffraction peak around 31.80° indicates a preferred oriented tetragonal phase with polycrystalline structure for all the doping concentrations in the host matrix. The peaks associated to the (131), (122), (221), 124), (016), (242), (423), (014) and (156) crystallographic planes were also observed. The XRD result implies that a single pure phase of $Tl_{10-x}Sb_xTe_6$ is obtained in the present study. Further, the particle size of the prepared samples was estimated using Debye-Scherrer formula,

$$(D = 0.9\lambda/B\cos\theta)$$

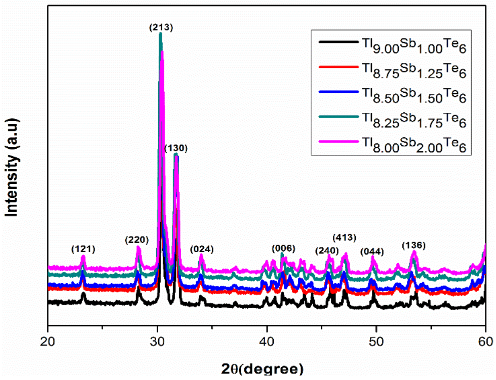

Fig. 1.Room temperature powder XRD pattern of $Tl_{10-x}Sb_xTe_6$ (x = 1, 1.25, 1.50, 1.75, 2).

The crystallite size value of the prepared samples is in the range (20-24 nm) indicating that Sb incorporations in $TlSbTe_2$ do not affect significantly its crystallite size. The XRD data are summarized in Table 1.

Table 1. Value of crystallite size and crystal system.

Sample	Crystallite size, D = 0.9λ/βcosθ (nm)	Lattice constant a, b ,c = (Å)	Volume (Å^3)
$Tl_9Sb_1Te_6$	24.247	a = b = 8.8931 c = 13.0052	1004.521
$Tl_{8.75}Sb_{1.25}Te_6$	21.795	a = b = 8.84510 c = 13.07515	1023.925
$Tl_{8.50}Sb_{1.50}Te_6$	21.180	a = b = 8.82510 c = 13.00010	1013.425
$Tl_{8.25}Sb_{1.75}Te_6$	21.128	a = b = 8.81010 c = 13.0010	1009.091
$Tl_8Sb_2Te_6$	20.455	a = b = 8.84814 c = 13.16215	1022.712

As X-ray diffraction techniques alone cannot find the exact ratio of elements present in the final product, some of supporting elemental analysis is used to enhance these diffraction techniques. EDX show quantitative percentage or ratio of the elements present in the samples. For $Tl_9Sb_1Te_6$ sample has a pure phase highly rich in thallium (69.9 % Tl, 25.8 % Te, 4.2 % Sb) for every element the atomic percent at different spots of various crystal for a special sample has averaged and related to the nominated atomic percent of the corresponding compound. In Fig. 2, the spectra show the Tl: Te ratio and the Sb concentration appear in the compound.

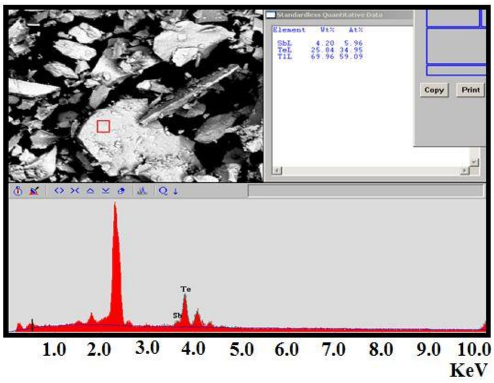

Standardless Quantitative Data

Element	Wt%	At%
SbL	4.20	5.96
TeL	25.84	34.95
TlL	69.96	59.09

Fig. 2 Image of Energy Dispersive X-ray spectroscope.

The electrical conductivity, **σ**, for $Tl_{10-x}Sb_xTe_6$ samples (where$1.0 \leq x \leq 2.0$) in the temperature range 300 K and 550 K is shown in Fig. 3. Electrical conductivity decreases gradually with increasing temperature, which shows similar trend to Tl_9BiTe_6 system. This behavior of our Sb doped system is true in case of intrinsic semiconductors with x= 1 as well as for doped semiconductors with x up to 2, like the compounds $Tl_{10-x}Sn_xTe_6$ and $Tl_{10-x}Bi_xTe_6$ [6, 8]. The decreasing behavior of electrical conductivity with temperature indicates the p-type conductivity.

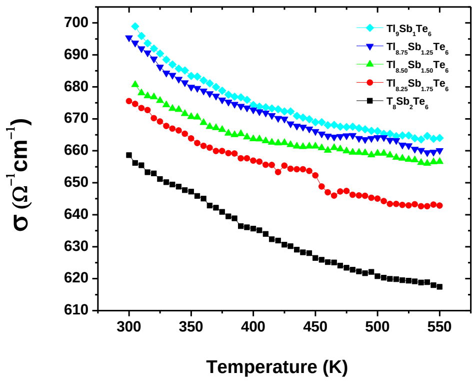

Fig. 3. Electrical conductivity of $Tl_{10-x}Sb_xTe_6$ with x varying between 1 and 2.

$Tl_9Sb_1Te_6$ has the highest electrical conductivity of 700 $\Omega^{-1}cm^{-1}$ at 300 K, which decreases gradually with increasing temperature, i.e. 661 $\Omega^{-1}cm^{-1}$ 550 K (Fig. 3). The electrical conductivity for $Tl_{10-x}Sb_xTe_6$ also decreases with increase in concentration of x. As an example in varying concentration of x from 1 to 2, the electrical conductivity, decreased from 700 $\Omega^{-1}cm^{-1}$ to 656 $\Omega^{-1}cm^{-1}$ at 300 K. Similarly at 550 K, it decreased from 661 $\Omega^{-1}cm^{-1}$ at x = 1 to 615 $\Omega^{-1}cm^{-1}$ at x = 2.

Table 2. The electrical conductivity at 300 and 550 K for all samples ($1.0 \leq x \leq 2.0$).

Sample	Electrical conductivity($\Omega^{-1}cm^{-1}$) at 300 K	Electrical Conductivity ($\Omega^{-1}cm^{-1}$) at 550 K
$Tl_9Sb_1Te_6$	700	661
$Tl_{8.75}Sb_{1.25}Te_6$	693	657
$Tl_{8.50}Sb_{1.50}Te_6$	679	653
$Tl_{8.25}Sb_{1.75}Te_6$	672	640
$Tl_8Sb_2Te_6$	656	615

See-beck coefficient (S) for $Tl_{10-x}Sb_xTe_6$ systems with various concentration of Sb (x=1.0, 1.250, 1.50, 1.750, 2.0) is shown in Fig. 4. All samples show an increasing trend of Seebeck coefficient with increasing temperature for example, for sample $Tl_8Sb_2Te_6$ it increased from S = 80.95 μVK^{-1} at 300 K to S = 126.93 μVK^{-1} at 550 K. In the same way for $Tl_9Sb_1Te_6$ compound the See-beck coefficient increased from S = 46.76 μVK^{-1} at 300 K to 82 μVK^{-1} at 550 K.

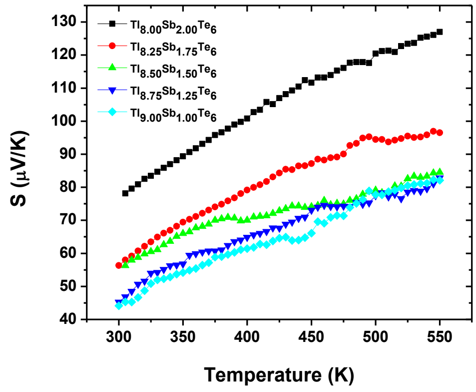

Fig. 4. See-beck coefficient of $Tl_{10-x}Sb_xTe_6$ with different concentration.

The See-beck Coefficient significantly increased upon Sb doping. At 300 K, it is enhanced from S = 46.76 μVK^{-1} at x = 1 to S = 80.95 μVK^{-1} at x =2. Similarly, in increasing Sb composition from x = 1 to 2, S increased from 82 μVK^{-1} 126.93 μVK^{-1} at 550 K.

P-type deficiency is frequently observed in such heavy metal telluride's, as also found in $Tl_{10-x}Ln_xTe_6$ series and Tl_9BiTe_6, causing a high number of charge carriers (> 10^{19} cm^{-3}) [7]. $Tl_{10-x}Ln_xTe_6$ series (Ln = La, Ce, Pr, Nd, Sm, Gd, Tb) having almost similar trend of See-beck coefficient of $Tl_{10-x}Sb_xTe_6$, increasing of See-beck coefficient with temperature by the creation of smaller energy band gaps (E_g), which can be easily excited from the valance band to conduction band.

The different temperature dependencies with variation in concentration *x*, can be attributed to the relationship between Seebeck coefficient and temperature and charge carrier concentration according to the following formula [17],

$$S = T\ \frac{8\pi^2 k^2{}_B m^*}{3eh^2}\left(\frac{\pi}{3n}\right)^{2/3}$$

Where,
k_B = Boltzmann constant,
e = electron charge,
h = Planck constant,
*m** = effective mass,
n = charge carrier concentration in system

The above equation shows that, *S* is directly proportional to *T*, but at the same time, it is inversely proportional to *n*; therefore, overall S would depend on which parameter dominates in a particular situation. Compounds with $x \geq 1$ is supposed to be p-type semiconductor as Tl_9SbTe_6 is formally an intrinsic semiconductor as observed from the experimental positive value of *S*.

As electrical conductivity,σ, rises with increases in *n* according to the equation $\sigma = n\,\mu e$, where μ = carrier mobility and *e* = charge of carriers and as mentioned above, *S* has $n^{-2/3}$ dependence, *S* and σ are related inversely through *n*. Therefore, supposedly, the opposite observationis expected for the σ trend. The experimental results endorse this expectation: as *x* increases, σ decreases for a given Sb due to decrease in *n* (see Fig. 3). Furthermore, as *T* increases, σ decreases, because $\mu = \tau / m^*$ where τ is the relaxation time, which decreases with increasing temperature.

Table 3. See-beck coefficient of all $Tl_{10-x}Sb_xTe_6$ samples at 300 and 550 K.

Sample	See-beck coefficient(μVK^{-1}) at 300 K	See-beck coefficient(μVK^{-1}) at 550 K
$Tl_9Sb_1Te_6$	46.76	82
$Tl_{8.75}Sb_{1.25}Te_6$	50.47	82.96
$Tl_{8.50}Sb_{1.50}Te_6$	58.75	84.5
$Tl_{8.25}Sb_{1.75}Te_6$	60.78	96.59
$Tl_8Sb_2Te_6$	80.95	126.93

4. Power factor

The power factor, characterized by $\alpha^2\sigma$, shows overall electrical performance of thallium antimony telluride. The power factor values of all samples are increasing with increasing the temperature. The increasing values of thallium antimony telluride sample are mainly attributed to increasing in See-beck coefficients. The Sb containing materials show a clear high value between 1.29μW-cm^{-1}K^{-2} and 9.78μW-cm^{-1}K^{-2} at 300 K and 550 K respectively with respect to un-doped sample. The samples with x = 1.0,1.250 and 1.50 show slight increasing with less dependence of temperature and aggregate at same point at 4.2 μW-cm^{-1}K^{-2} as shown in Fig. 5. All Sb samples investigated here have shown better performance of power factor. Tl_9LnTe_6 series was reported that the doping of different elements i.e (Ce, Pr) in ternary group show different values of power factor occur in the range of 2.9-4.7 μWcm^{-1}K^{-2}at 550K. Ternary group ($Tl_{10}SnTe_6$) substitute of Sn has reported the value of power factor at x = 2.05 are 3.8-4.97 μWcm^{-1}K^{-2} at 320 K and 685 K respectively [18] which is quite low value compared to the one reported in the present study, i.e. for $Tl_8Sb_2Te_6$ power factor is 8.98μWcm^{-1}K^{-2} at 550 K.

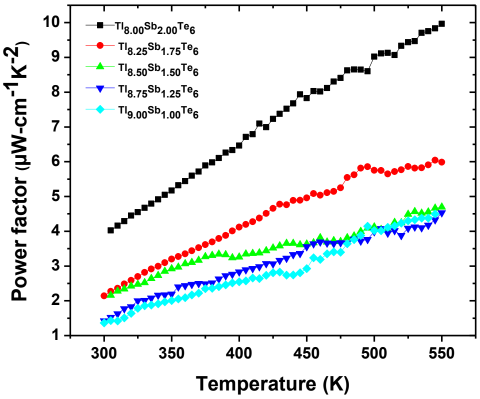

Fig. 5. Power factor of $Tl_{10-x}Sb_xTe_6$.

4. Conclusions

We have studied the thermoelectric properties of $Tl_{10-x}Sb_xTe_6$compound (with x = 1.0, 1.250, 1.50, 1.750, 2.00), doped with p-type antimony element on Thallium Telluride group. Thallium Antimony Telluride nanocrystal were prepared by using ball milling techniques and then through hot-pressing we made a dense pellet to measure thermoelectric properties. Structural and compositional analyses of ($Tl_{10-x}Sb_xTe_6$) were carried out with the help of X-Ray diffraction (XRD) and Energy Dispersive X-ray Spectroscope (EDX). XRD pattern shows that thallium antimony telluride nanocrystals are showing tetragonal structure with space group (*I4/mcm*).

The substantial increment in the Seebeck coefficient (*S*) was achieved in 'Sb' system on the cold-pressed and hot-pressed $Tl_{10-x}Sb_xTe_6$, i.e. at 300 K, we observed 'S' values of 78.1 μVK^{-1} for $Tl_8Sb_2Te_6$ and 126μVK^{-1} at 500 K respectively. All these compound shows p-type behavior, as they have positive Seebeck coefficient. Therefore, greater the 'Sb' value lower the electrical conductivity and high the Seebeck coefficient. The high Seebeck coefficient in turn gave the enhanced value of power factor. We concluded that the relative higher values of 'Sb' based compound made them interesting for further study and practical application, i.e. to fabricate high efficient thermoelectric generator.

References

[1] M. G. Kanatzidis, Chem Mater. **22**, 648 (2010).
[2] A. D. LaLonde, Y. Z. Pei, H. Wang, G. J. Snyder, Mater Today **14**, 526 (2011).
[3] J. R. Sootsman, D. Y. Chung, M. G. Kanatzidis, Angew Chem. Int. Ed. **48**, 8616 (2009)
[4] G. S. Nolas, D. T. Morelli, T. M. Tritt, Annu. Rev. Mater. Sci. **29**, 89 (1999).
[5] J. Yang, W. Zhang, S. Q. Bai, Z. Mei, L. D. Chen, Appl. Phys. Lett. **90**, 108 (2007).
[6] R. Chen, A. I. Hochbaum, R. D. Delgado, W. Liang, E. C. Garnett, M. Najarian, A. Majumdar, P. Yang, Enhanced thermoelectric performance in rough silicon

nanowires, in: APS Meet., 2008. <http://meetings.aps.org/Meeting/MAR08/Event/77251> (accessed December 4, 2017).

[7] A. I. Boukai, Y. Bunimovich, J. Tahir-Kheli, J. Yu, W. A. I. Goddard, J. R. Heath, Nature **451**, 168 (2008).

[8] R. Venkatasubramanian, E. Siivola, T. Colpitts, B. O'Quinn, Nature **413**, 597 (2001).

[9] B. Poudel, Q. Hao, Y. Ma, A. Minnich, A. Muto, Y.C. Lan, B. Yu, X. Yan, D. Z. Wang, D. Vashaee, Science **320**, 634 (2008).

[10] A. Shakouri, C. Labounty, P. Abraham, J. Piprek, J. E. Bowers, Materials Research Society Proceedings **545**, 449 (1999).

[11] D. Vashaee, A. Shakouri, Phys. Rev. Lett. **92**, 106103/1 (2004).

[12] G. J. Snyder, E. S. Toberer, Nat. Mater. **7**, 105 (2008).